

# Extended Thermoelastic Stress Analysis Applied to Carbon Steel and CFRP

Robin PLUM<sup>\*</sup>, Justus MEDGENBERG<sup>\*\*</sup>, Marco MERZBACHER<sup>\*\*\*</sup>,  
Thomas UMMENHOFER<sup>\*</sup>

<sup>\*</sup> Karlsruhe Institute of Technology, Research Center for steel, timber and masonry,  
Otto-Ammann-Platz 1, 76131 Karlsruhe, Germany;  
robin.plum@kit.edu, thomas.ummenhofer@kit.edu

<sup>\*\*</sup> Bilfinger Berger AG, Carl-Reiß-Platz 1-5, 68165 Mannheim, Germany;  
justus.medgenberg@bilfinger.de

<sup>\*\*\*</sup> Merzbacher UB, Odastr. 3, 38122 Braunschweig, Germany;  
info@merzbacher-ub.de

**Abstract.** Thermoelastic Stress Analysis (TSA) by means of radiometric full field measurements has been primarily developed over 20 years ago. Although the underlying physics concerning the linear thermal response with respect to the loading as well as dissipative and nonlinear effects have been extensively studied in the past the potential of applications in the field of non destructive testing does not seem to be exhausted, yet. As an extension of the classic thermoelastic analysis the use of second harmonic temperature amplitudes for spatially resolved damage detection due to cyclic plasticity in ferritic low-alloy carbon steel is demonstrated. Temperature variations of several mK are found to be useful as a fatigue damage indicator. Furthermore the application to partially delaminated CFRP coupons under cyclic peeling load reveals that the classic thermoelastic measurement is able to visualise the locally stressed woven fibre ply. In contrast, the evaluation of the spatial temperature response at the double loading frequency clearly allows to detect the delamination front of homogeneous coupons whereas the dominating bending stress distribution is efficiently suppressed.

## Introduction

Besides of the established NDT methods competitive new approaches based on modern infrared thermography and image processing have been widely accepted in many fields of engineering. Today, especially the progress and application of active thermography methods utilizing optical, ultrasonic or eddy-current stimulation represent focus areas of numerous research groups.

As a complementary method, the Thermoelastic Stress Analysis (TSA) of structural members under low frequency mechanical loading contributes to further understanding of material specific damage mechanisms since load redistributions in components made of homogeneous steel and anisotropic woven FRPs are measured in full-field. However, several investigations reveal that dissipative effects which typically accompany progressive damaging show up as a nonlinearity in the acquired infrared records [1, 2, 3]. For metals cyclic plasticity and crack closure contribute to a significant thermal response at the second harmonic frequency of the loading. The work of Huß [2] manifests that geometrical nonlinearities can exceed the thermal signature of material nonlinearities by far. Thus it can be presumed that besides of fatigue cracks in steel components delaminations in fibre reinforced materials can be identified by the same TSA based approach.

## Thermoelastic and Dissipative Temperature Variation

The thermal state of a solid is coupled to the mechanical loading and vice versa. In the context of Thermoelastic Stress Analysis the influence of the dynamic stress state on the thermal response is of interest. The general form of the heat equation of a deformable solid body is derived from the conservation of energy and reads in local form [4].

$$\rho C_\varepsilon \frac{dT}{dt} - \frac{\partial}{\partial x_j} \left( k \frac{\partial T}{\partial x_j} \right) = \rho r + \sigma_{ij} \frac{\partial \varepsilon_{ij}}{\partial t} - \rho \frac{\partial \Psi}{\partial V_k} \frac{dV_k}{dt} + \rho T \frac{\partial^2 \Psi}{\partial T \partial V_k} \frac{dV_k}{dt} \quad (1)$$

In equation (1) the Einstein summation convention has been used.  $\rho$  denotes the density,  $C_\varepsilon$  is the heat capacity at constant strain,  $T$  is the absolute temperature,  $k$  is the thermal conductivity tensor,  $\varepsilon_{ij}$  and  $\sigma_{ij}$  are the strain and the stress tensor, respectively,  $r$  is an internal heat source per unit mass and  $\Psi$  is the Helmholtz free energy depending on  $k$  independent internal state variables  $V_k$ .

On this basis the 3-dimensional heat conduction equation including thermoelastic and thermoplastic heat generation can be derived with the assumption of linear elastic material behaviour, isotropic and constant material coefficients that are temperature independent (compare [5]).

$$\rho C_\varepsilon \dot{T} - k \nabla^2 T = T_0 \left( -\frac{E\alpha}{1-2\nu} \right) \dot{\varepsilon}_1^e + \alpha_p \sigma_{ij} \dot{\varepsilon}_{ij}^p \quad (2)$$

Here,  $\varepsilon_1^e$  denotes the first invariant of the elastic strain tensor,  $\varepsilon_{ij}^p$  the irreversible part of the strain tensor,  $\alpha$  the thermal expansion coefficient,  $E$  the Young's modulus,  $\nu$  the Poisson's ratio and  $T_0$  the initial temperature. The dimensionless coefficient  $\alpha_p$  is the ratio of plastic work that is converted to heat and the total plastic work.  $\alpha_p$  is typically very close to 1.0 since only a small fraction of the plastic work (the stored energy of cold work) is used for altering the inner material properties e.g. the density of dislocations or the hardening state.

Neglecting the heat diffusion and plastic deformation leads to the well known equation of linear thermoelasticity at adiabatic conditions.

$$\dot{T} \approx -\frac{\alpha}{\rho C_p} T_0 \dot{\sigma}_1 \quad (3)$$

Here, higher order terms are ignored and the transition from  $C_\varepsilon$  to  $C_p$  (the heat capacity at constant pressure) is made.  $\sigma_1$  is the first invariant of the stress tensor.

## Thermographic Measurement and Data Processing

In earlier works [6, 1] it has been shown that the onset of cyclic plastic deformations in steel specimens leads to a significant generation of a thermal response at the second harmonic of the loading frequency. Therefore a specialised data processing was developed. During high cycle fatigue testing infrared sequences are acquired using a cooled 640 x 512 pixel focal-plane infrared camera FLIR Phoenix DTS which offers a high thermal sensitivity (NETD  $\approx$  20 mK) and high frame rates at the same time.

As a first step of the data processing, a two-point non-uniformity correction and a bad pixel replacement are conducted. In order to compensate for specimen movements

which blur the IR images a motion compensation algorithm based on the two-dimensional cross-correlation is applied. Although there is no strain compensation this measure leads to almost perfectly stable IR sequences.

Next, a point of the specimen is chosen which is known to behave purely elastic. The IR pixel signal of this location is referred to as the linear reference signal. Due to the thermomechanical coupling this signal directly corresponds to the applied loading. The reference signal is now shifted in phase and scaled in magnitude pixel by pixel to fit to every other signal in the sense of a least-square minimisation. This procedure results in the amplitude and phase mappings at the loading frequency as it is known from TSA measurements. Existing nonlinearities in the temperature signal due to cyclic plasticity are assessable by evaluating the difference signal between the fitted reference signal and the original pixel signal. A nonlinear temperature amplitude is introduced by fitting a sine curve with the double frequency to the difference signal. Figure 1 shows the concept of the data processing. Theoretically the amplitude and phase values at the base frequency and at the second harmonic can also be achieved by applying a discrete Fourier Transform to the IR sequence. However, tests revealed that the proposed data processing leads to better results [1]. Furthermore, the procedure can be used in case of non perfect sinusoidal loading. Even in the case of random loading the evaluation of the RMS value of the difference signal instead of the nonlinear sine-based amplitude can show reasonable results [7].

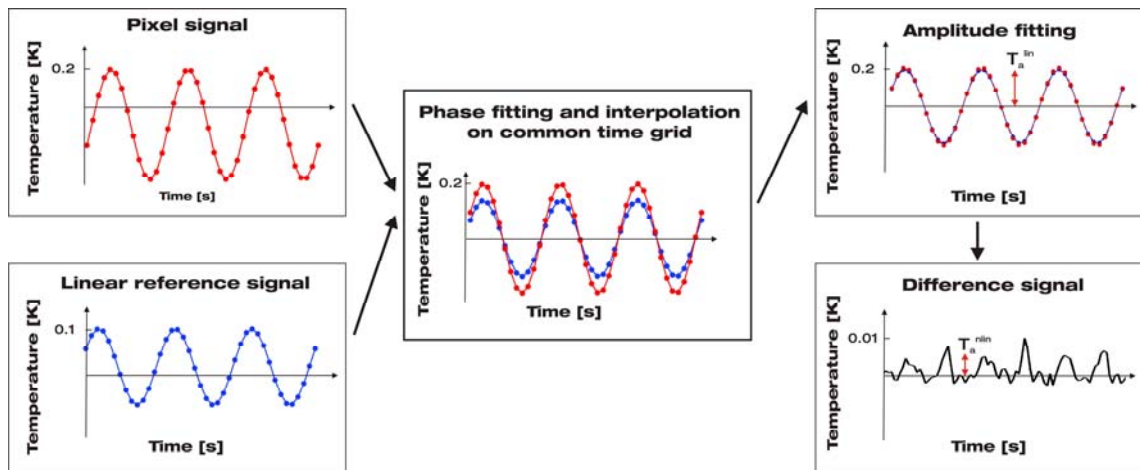
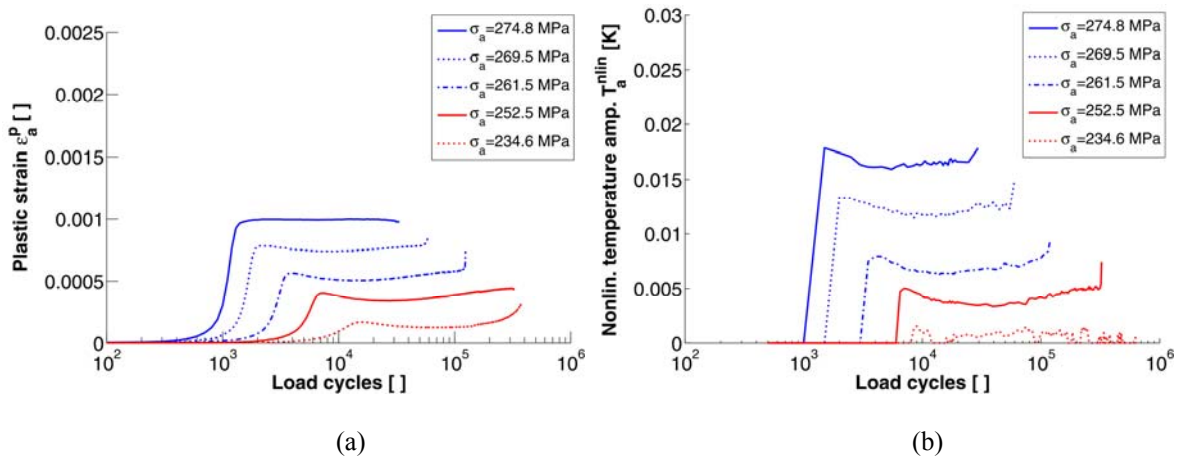


Figure 1. IR data processing

## Investigation of Carbon Steel Samples

The proposed measurement and data processing was applied to cylindrical specimens made from mild carbon steel S355J2+N, first. Several one axial fatigue tests at constant amplitude and  $R = -1$  were performed. During the test runs a series of infrared sequences of about 2000 images each was acquired. The camera frame rate has been set to 412 Hz which results in a reasonable oversampling of the 2.5 Hz loading frequency. The smooth specimens have been equipped with strain gauges which were monitored during the tests as well. Figure 2a depicts the plastic strain history of five specimens tested at different load levels. The different stages of primary softening, hardening and secondary softening which are typical for the used steel grade are clearly resolved. As a direct comparison figure 2b shows the history of the evaluated nonlinear temperature amplitude averaged over an expanded range of interest.

The onset of increasing plastic strains in terms of the load cycle number as well as the cyclic material behaviour is very well reproduced by the thermographical approach.



**Figure 2.** Evolution of plastic strain (a) and nonlinear temperature amplitude (b)

The described methodology was also applied to mildly notched steel samples. Figure 3 illustrates a rendering of the specimen type. The geometrical notch at the center of the cylindrical specimen results in a local stress concentration (factor 1.35). Due to that the onset of cyclic plasticity and the accumulation of fatigue damage will be strongly localised and limited to the hot-spot. As another consequence of the stress concentration the assumption of adiabatic conditions is not valid. Thus, the loading frequency strongly influences the linear temperature amplitudes achieved by TSA measurements. Here, a higher loading frequency leads to a higher thermoelastic signal. This has been proven by numerical as well as experimental analyses [6, 1].

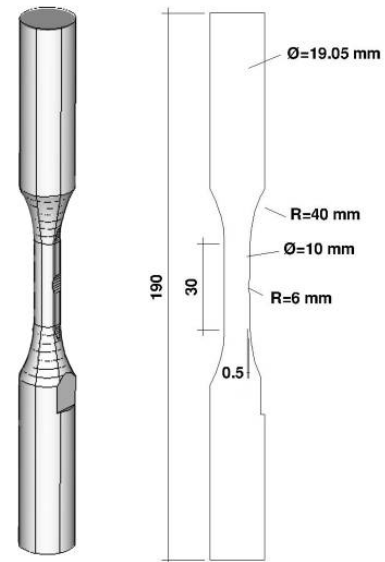


**Figure 3.** Notched steel specimen

However, the loading frequency of the available hydraulic testing machine is limited to 25 Hz depending on the displacement amplitude. The notched steel specimens have been fatigue tested until complete failure using  $R = -1$  at a loading frequency of 15 Hz. The load amplitude was adjusted by means of a FE simulation so that the notch bottom was stressed no more than 85 % of the static yield limit.

The IR sequences were processed as described above. Figure 4 shows the distribution of the linear (top) and nonlinear temperature amplitude (bottom) in the notch region at different relative lifetimes  $N/N_f$  where  $N$  is the cycle number and  $N_f$  the number of cycles to failure. The  $x$  and  $y$  location (0/0) corresponds to the center of the notch, the  $x$ -axis is the longitudinal axis of the specimen. At the left side of the notch bottom a rectangular area was not available for the IR measurement since it was used for parallel microscopic imaging. From the thermoelastic response in figure 4a we can conclude that the notch clearly acts as a stress raiser and the edges above and below are less strained. Nonlinearities in the thermal response can be found after 10 % of the specimen lifetime at the notch bottom indicating that cyclic plasticity occurs. The initiation of a macroscopic

crack typically occurs at  $N/N_f=0.85$  which can be visualised by a local drop of the thermoelastic temperature amplitude and a strong increase of the nonlinear response (figure 4b). During macroscopic crack propagation the nonlinear thermal response is excessively amplified due to crack opening and closure [2]. At this time the crack region cannot transmit the axial loads any longer. As a result the thermoelastic signal decreases and load redistributes towards the outer region as can be identified in figure 4c.

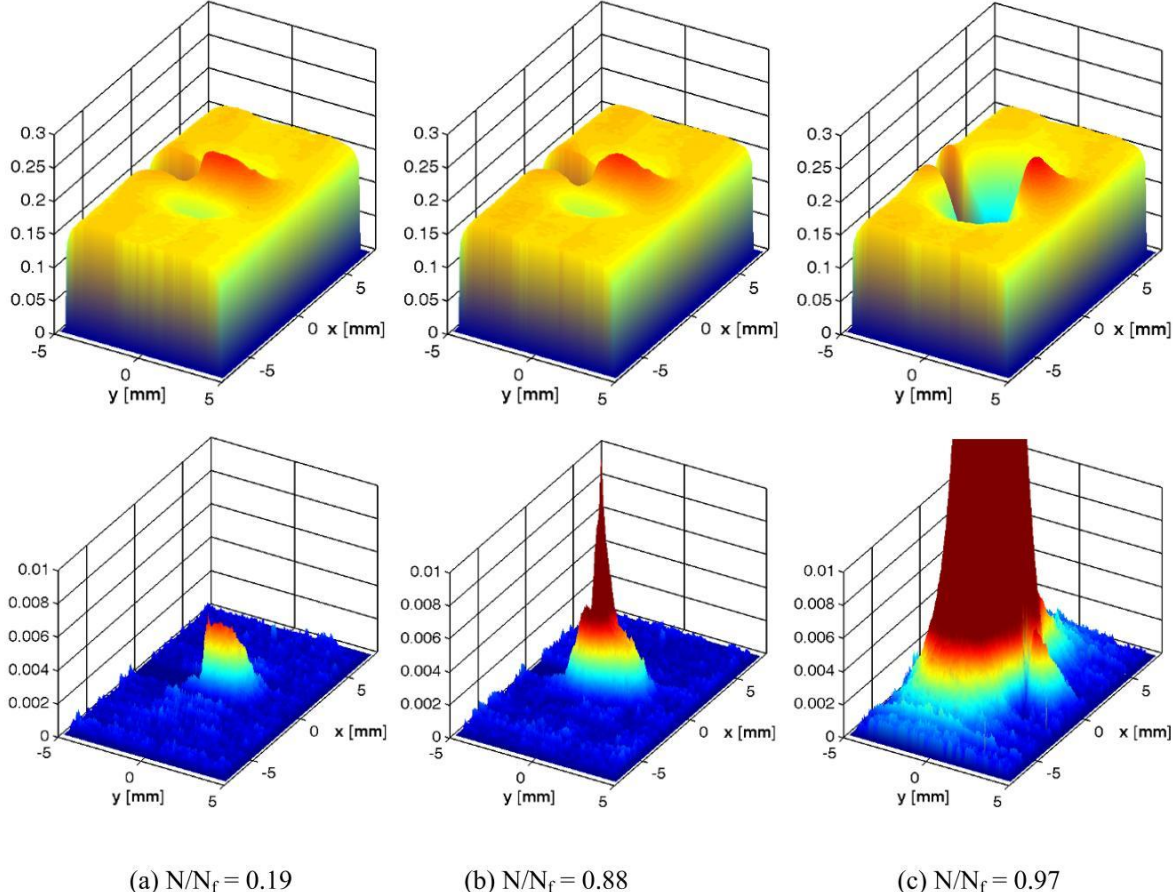


**Figure 4.** Distribution of linear elastic (top) and nonlinear (bottom) temperature amplitudes

**Investigation of CFRP Samples**

Although the presented methodology was originally developed for identification of a nonlinear thermal response of metals it was also applied to two different types of CFRP samples featuring an artificial delamination. The coupon shown in figure 5 is based on a woven fabric embedded in a polymer matrix.



**Figure 5.** CFRP coupon with artificial delamination

The initial delamination at one half of the specimen's length was realised by an inserted Teflon film during fabrication. A common method for evaluating the resistance against further delamination is the DCB test (Double Cantilever Beam test). Figure 6 depicts a mounted specimen that is based on an unidirectional laminate, i.e. all fibres of one ply are parallel. All samples were coated with a graphite spray in order to achieve a homogeneous and high emissivity surface. Additionally a high contrast marker which allows for motion compensation of the IR records was attached to the specimen.

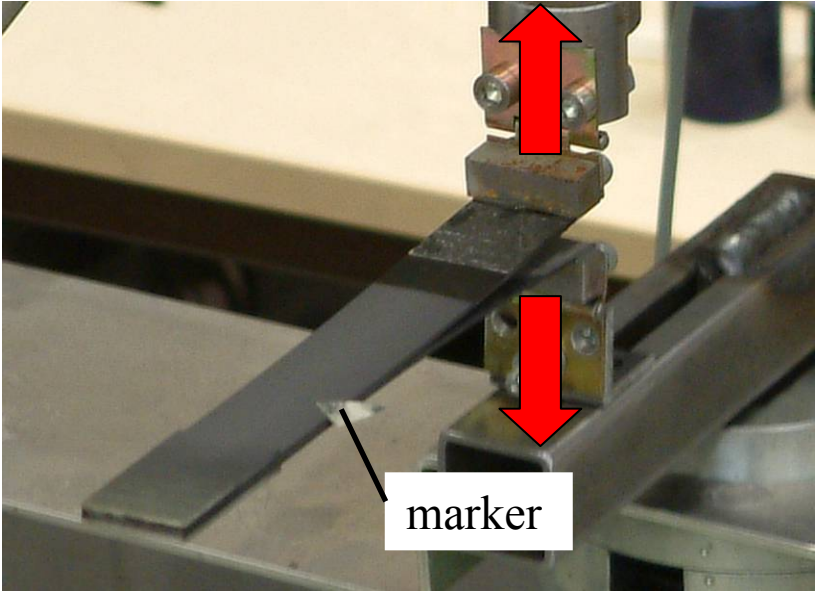


**Figure 6.** T-peel testing of the coated CFRP specimen

Fatigue loading of the CFRP coupons was conducted at different frequencies in order to investigate the influence on the thermoelastic signal strength. The infrared camera was positioned above the specimen pointing at the transition zone of the half delaminated coupon. As can be seen from figure 7 the delaminated region (bottom) can be easily distinguished from the part which is of full integrity (top). Clearly, the two delaminated fringes are loaded in the sense of cantilevers which are fully restrained at their junction. Thus, the undamaged 4 mm thick part of the specimen is nearly not stressed at all during the test.

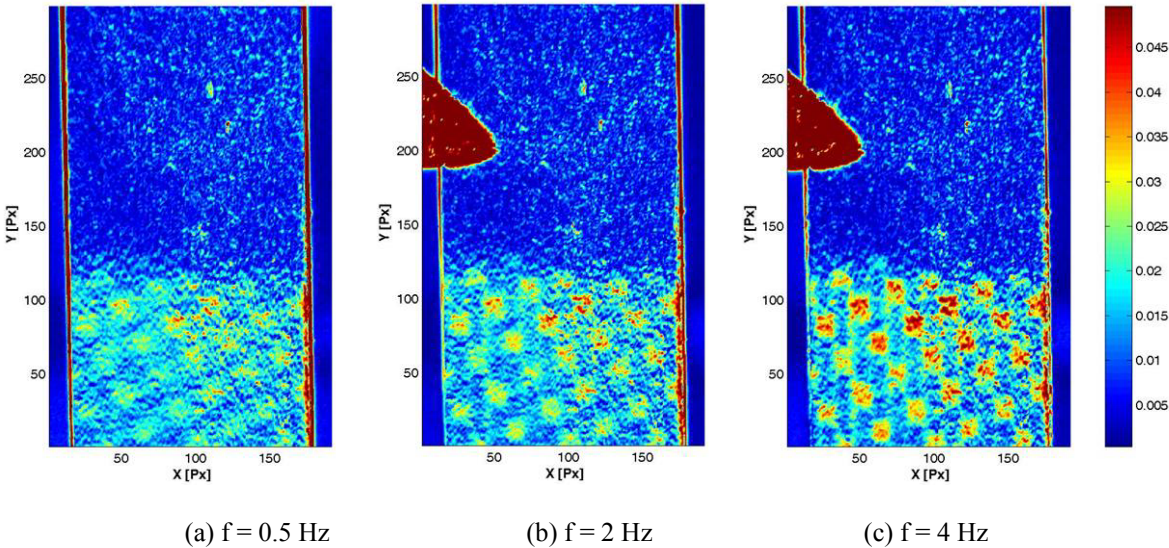


**Figure 7.** Distribution of the linear elastic temperature amplitude

The benefit of the proposed data processing was best in case of the unidirectional laminate specimen. Figure 8a shows the linear elastic temperature amplitude mapping for a similar specimen preparation. The distribution essentially corresponds to the gradual bending stress distribution which is minimal at the hinged joint where the varying force is acting and maximal at the junction of both fringes. In contrast to this result an evaluation of the nonlinear temperature amplitude yields the mapping in figure 8b. Here, the bending stress distribution is completely suppressed. Instead, the delamination front itself is clearly visible due to its geometrically nonlinear behaviour. An additional hot-spot on the right side attracts attention which is probably indicating another independent defect in the upper fringe.

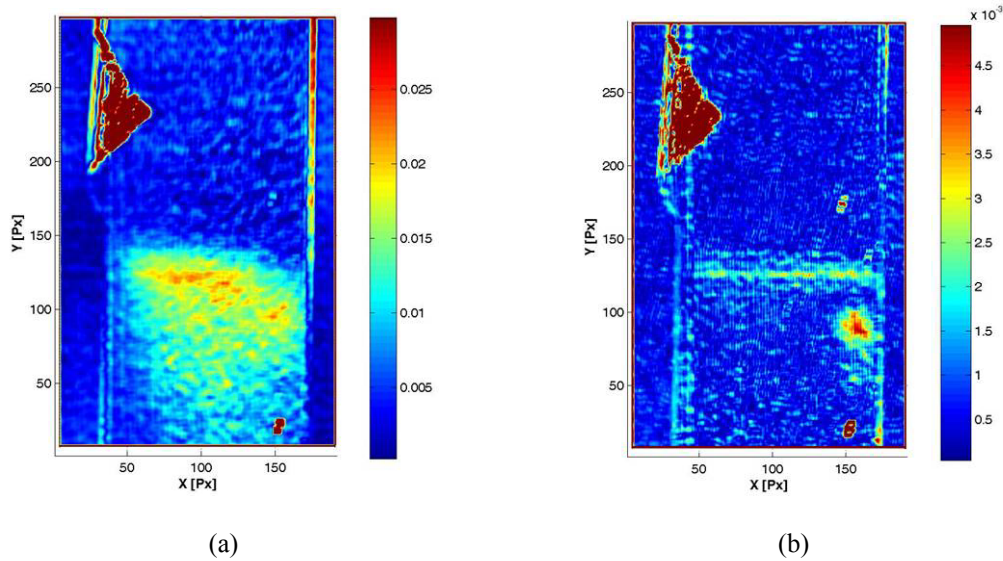


**Figure 8.** Temperature amplitude at the loading frequency (a) and at the double frequency (b)

## Conclusions

The present work demonstrates the benefits of a second harmonic evaluation based on TSA records. In the case of notched small scale steel specimens subjected to high cycle fatigue loading the recently developed post-processing methodology results in a direct visualisation of the damage progress. Here, the nonlinear temperature amplitude mapping complements the distribution of the linear elastic response. It was found that the proposed method is sensitive to periodic temperature deviations from a reference signal shape in the order of a few mK.

The application to CFRP coupons subjected to DCB testing resulted in a clear detection of the delamination front which qualifies the extended Thermoelastic Stress Analysis for defect detection in the field of composite materials used in the aerospace industry.

Clearly, TSA based methods are especially suited to be applied to fatigue tests under laboratory conditions. Besides of the complementation and verification of numerical simulations by mapping the thermoelastic signal the evaluation of the second harmonic response brings further insight into the component's damage state.

Thermoelastic Stress Analysis whose basics are well known will probably gain more attention in the field of material testing since the use of fibre reinforced light-weight materials or multimaterial systems for load bearing structural components is increasing and the failure mechanisms become more complex.

## References

- [1] Medgenberg, J.: "Investigation of localized fatigue properties in unalloyed steels by infrared thermography". Dissertation, Technische Universität Braunschweig, Braunschweig, 2008.
- [2] Huß, A.: "Rißdetektion und -bewertung mit dem Verfahren der Thermoelastischen Spannungsanalyse". Fortschrittsberichte VDI, Reihe 18, No. 147, Düsseldorf, VDI-Verlag, 1994.
- [3] Krapez, J.C, Pacou, D.: "Thermography detection of damage initiation during fatigue tests". Proceedings of SPIE Vol. 4710, pp. 435-449, 2002.
- [4] Lemaitre, J., Chaboche, J.L.: "Mechanics of solid materials". Cambridge University Press, 1990.
- [5] Nowinski J.L.: "Theory of thermoelasticity with applications". Noordhoff International Publishing, Alphen aan den Rijn, 1978.
- [6] Ummenhofer, T., Medgenberg, J: "Numerical modelling of thermoelasticity and plasticity in fatigue-loaded low carbon steels. Studies for a thermographic approach". Qirt Journal Vol. 3, No. 1, pp. 71-92, 2006.
- [7] Ummenhofer, T., Plum, R.: "Bestimmung des inhärenten Schadens ermüdungsbeanspruchter Stahlbauteile mit aktiver Thermografie". Sonderforschungsbereich 477, TU Braunschweig, Tagungsband, pp. 77-82, 2010.